Resonance in a piezoelectric material

Daniel L. Tremblay

Physics Department, The College of Wooster, Wooster, Ohio 44691

May 8, 2006

An AC voltage was used in conjunction with a piezoelectric material consisting of lead, titanium, and zirconium to investigate the resonant mechanical frequencies and patterns of the piezoelectric sample. Both longitudinal and flexural oscillatory modes were examined. Resonant frequencies were found at ~42.1 x 10^3 rad./s, ~96.1 x 10^3 rad./s, and ~135.7 x 10^3 rad./s. These resonant frequencies correspond to the first flexural mode, second flexural mode, and first longitudinal mode respectively. Further investigation is needed to verify the model being used for the overall resonant frequencies. However, this model enabled the speed of sound in the piezoelectric sample to be determined as (3291 ± 6) m/s. In addition, two methods were used in modeling a particular resonance in greater detail. Analyzing the amplitude and phase shift of oscillation yielded a resonant frequency as well as damping coefficient which correspond to a Q factor of (25.30 ± 0.13).

INTRODUCTION

The piezoelectric effect was discovered by Pierre and Jacque Curie in 1880. Electric polarization, and thus a potential difference, is created when mechanical stress is placed upon a piezoelectric sample. This is the direct piezoelectric effect as opposed to the converse piezoelectric effect, which is the creation of strain on a sample when a potential difference is created across the sample. The Curies eventually discovered that the piezoelectric coefficient for a quartz crystal is the same for both the direct and converse piezoelectric effects[1].

THEORY

Piezoelectricity is simply the means by which we can examine the mechanical resonance of a piezoelectric sample. The resonance relevant in this experiment is derived from the differential equation of a forced, damped harmonic oscillator

$$\ddot{x} + 2\beta\dot{x} + \omega_0^2 x = A\cos(\omega t) \tag{1}$$

where β is the damping coefficient, ω_0 is the natural oscillating angular frequency, ω is the angular frequency, and A is proportional to the amplitude of the driving force. The solution to this second order differential equation has two parts: a complementary and particular solution. The particular solution takes the form[2]

$$x_p(t) = D\cos(\omega t - \delta) \tag{2}$$

where δ is the phase angle between the driving angular frequency and oscillating angular frequency. D is[2]

$$D = \frac{A}{\sqrt{(\omega_0^2 - \omega^2)^2 + 4\omega^2\beta^2}} \tag{3}$$

Oscillations near a resonance point will occur with much greater amplitude.

The delay between the driving force and resulting motion is described by δ which is given by[2]

$$\delta = \tan^{-1}\left(\frac{2\omega\beta}{\omega_0^2 - \omega^2}\right) \quad (4)$$

As frequency approaches resonance, the phase angle will approach $\pi/2$. Equations 3 and 4 are the two ways in which resonance can be experimentally detected and measured.

The oscillations which lead to resonance can occur two ways in the rod. Longitudinal modes are to waves which travel up and down the length of the rod as a series of compressions and rarefactions. The frequencies of these modes can be given by[3]

$$f_n = n\frac{v}{2L} \quad (5)$$

where v is the speed of sound in the rod, L is the length of the rod, and n is 1, 2, 3, … .

The other mode of oscillation is flexural. These modes consist of the rod bending back and forth, with higher modes consisting of more nodes and antinodes. The frequencies of these modes are given by[3]

$$f_n \approx (2n+1)^2 \frac{\pi v R_G}{8L^2} \quad (6)$$

where R_G is the radius of gyration, and n is 1, 2, 3, … . The radius of gyration for a square rod with side length d is $d/\sqrt{12}$.

Even without any knowledge of the experimental setup, patterns in the resonant modes of the system can be determined with Equations 5 and 6. Dividing the equation for longitudinal modes by itself yields

$$\frac{f_n}{f_m} = \frac{n}{m} \quad (7)$$

where n and m are positive integers and represent different order resonant longitudinal modes. This same method can be employed with Equation 6

$$\frac{f_n}{f_m} = \frac{(2n+1)^2}{(2m+1)^2} \quad (8)$$

Since both longitudinal and flexural oscillations take place in the sample, it's important to be able to recognize their relationship

$$\frac{f_{long}}{f_{flex}} = \frac{4nL}{(2m+1)^2 R_G \pi} \quad (9)$$

where n is the order of the longitudinal resonant mode and m is the order of the flexural resonant mode.

EXPERIMENT

A simplified schematic of the experimental setup can be seen in Figure 4. An HP33120A Waveform Generator outputted a signal ranging from 500 Hz to 25 kHz (ω = 3.1 x 10^3 rad./s to 157.1 x 10^3 rad./s) and 1.0 V_{pp} to 4.0 V_{pp}. Since this signal was insufficient to adequately drive the piezoelectric sample, it was applied to a Kepco BOP 500M, which amplified by a factor of approximately 50 at low frequencies. At frequencies above approximately 1 kHz, the gain from the power amplifier rolled off. To compensate, the peak-to-peak voltage was increased at higher frequencies to ensure that the peak-to-peak voltage driving the piezoelectric sample was never below 30 V_{pp}. The signal from the power amplifier was measured by a Textronix TDS 2012 Oscilloscope, and was sent to the lead, titanium, zirconium piezoelectric sample. The sample was rectangular and measured 76.5 ± 0.2 mm by 9.6 ± 0.1 mm. The sample formed the basis of a stack which rested on an air table. Above the piezoelectric sample lay a PCB Force Transducer. The air table reduced mechanical noise.

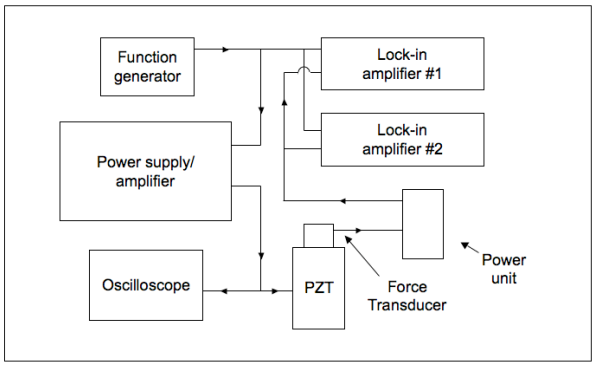

Figure 1: Simplified schematic of experimental setup.

The force transducer was capable of detecting forces via a piezoelectric, and thus was able to detect the strain of the piezoelectric sample. The signal from the force transducer was sent to a PCB 484B10 where it was amplified before being sent to two Stanford Research Systems SR510 Lock-In Amplifiers (LIA). The LIA also received the signal being output by the function generator as their reference inputs. The LIA were capable of taking the reference signal from the function generator and looking for a signal with the same frequency in the signal from the force transducer. When detecting the identical frequency in the force transducer, the amplitude of oscillation and phase angle were recorded. This information was displayed as components of the phase angle. In order to measure both components of the phase angle simultaneously, two LIA were necessary.

To take data, the function generator output a sine wave at 500 Hz with an amplitude of 1 V_{pp}. The frequency was increased in increments of 500 Hz to a maximum frequency of 25 kHz. As the frequency was increased, the output of the power amplifier decreased. Therefore, the voltage outputted by the function generator was increased by 1 V_{pp} whenever there was less than 30 V_{pp} driving the piezoelectric.

This overall, low-resolution resonance curve of the piezoelectric sample was used to locate the resonant frequencies. This data was then used to further investigate a resonant frequency at a higher resolution. Frequency was increased by 100 Hz increments when taking this data.

ANALYSIS AND INTERPRETATION

The overall amplitude resonance curve of the piezoelectric sample can be seen in Figure 2. Drastic increases in the amplitude of oscillations correspond to resonant frequencies at ~42.1 x 10^3 rad./s, ~96.1 x 10^3 rad./s, and ~135.7 x 10^3 rad./s.

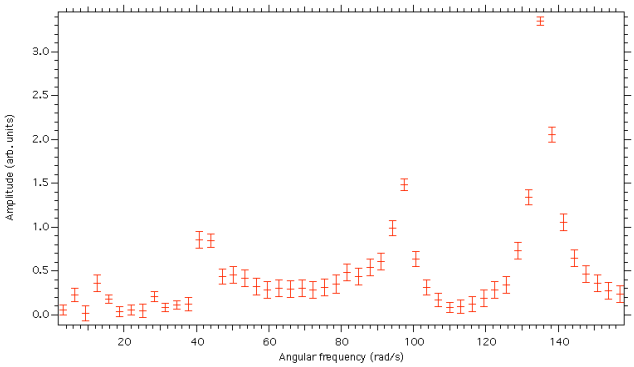

Figure 2: Amplitude resonance curve over a large range of frequencies.

Since Equations 7, 8 and 9 are in terms of frequency, not angular frequency, the discussion on resonant modes in the sample will be in terms of frequency. Thus, the three resonances in Figure 2 occur at ~6.7 kHz, ~15.3 kHz, and ~21.6 kHz. Equations 7, 8, and 9 can be used to determine resonant modes and also to predict resonant modes at higher frequencies.

Assuming that the ~15.3 kHz resonance is the second flexural mode, the other resonances can be determined. The ~21.6 kHz resonance becomes the first longitudinal mode, and the ~6.7 kHz resonance becomes the first flexural mode.

Mode	Theoretical value (kHz)	Experimental value (kHz)
Flexural = 1	5.507	~6.7
Flexural = 2	(15.3)	~15.3
Longitudinal = 1	21.510	~21.6

Table 1: Theoretical and experimental values for three observed resonances.

The speed of sound in the lead, titanium, and zirconium composite material can be determined from Equation 6 when the ~15.3 kHz is assumed to be the second flexural mode. The speed of sound was determined to be (3291 ± 6) m/s. However, this analysis is cursory without higher resolution data of the three resonances used.

When the stack was deconstructed to take physical measurements of the piezoelectric sample, a reconstruction of the stack did not produce similar resonance patterns as were initially present. However, Figure 3 shows a detailed resonance curve which was not disturbed by the reconstruction of the stack.

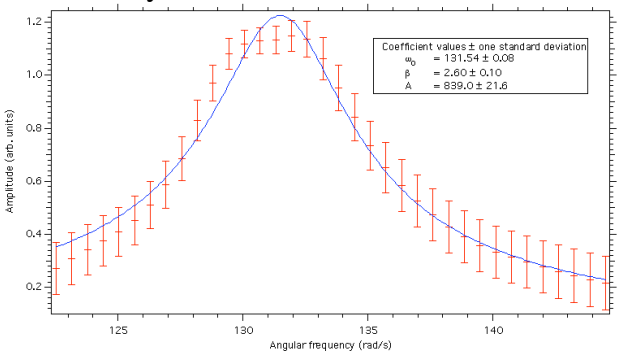

Figure 3: Amplitude resonance curve**.**

The amplitude resonance curve yielded values for ω_0 of (131.5 ± 0.1) x 10^3 rad./s, β of (2.6 ± 0.1) x 10^3 rad./s, and A of (839 ± 22) x 10^3 m/s^2. The speed of sound in the sample is found to be (3202.1 ± 0.1) m/s.

The phase angle can also be used to determine where resonance occurs. Equation 4 describes the phase shift between the driving force and oscillations. A resonant frequency can be found when the phase shift is π/2. Figure 10 shows the phase shift angle, δ, as a function of frequency. Experimentally, a resonance may not occur at a phase shift of π/2 due to previous resonances shifting the phase difference between the driving frequency and oscillations.

Igor Pro 5.04b was used to plot and analyze this data, but had difficulty in comparing this data to Equation 4, which describes the shift in phase angle around a resonant point. In order to analyze the phase shift data, it first had to be manipulated. Every data point had π/2 added to it so that Igor would process the trig functions as they went to a different quadrant, which was a possible problem to fitting the data for analysis. The tangent was then taken of Equation 4 which yielded

$$\tan\delta = \frac{2\omega\beta}{\omega_0^2 - \omega^2} = \frac{\text{Amp of } 90^\circ\text{LIA}}{\text{Amp of } 0^\circ \text{ LIA}} \qquad (10)$$

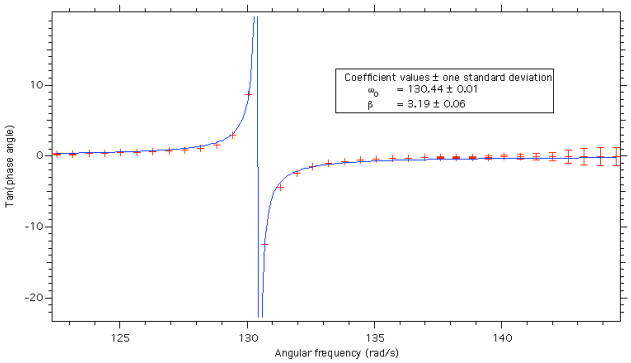

Figure 4: Manipulated phase angle data fit for analysis.

This analysis of the phase angle data gave ω_0 to be (130.44 ± 0.01) x 10^3 rad./s and β to be (3.2 ± 0.1) x 10^3 rad./s.

CONCLUSION

Resonance in a piezoelectric material was examined using the piezoelectric effect to induce mechanical oscillations. Resonant standing wave frequencies were found and modeled at ~42.1 x 10^3 rad./s, ~96.1 x 10^3 rad./s, and ~135.7 x 10^3 rad./s. The model which best describes the ratios of the resonant frequencies has the resonance at ~135.7 x 10^3 rad./s corresponding to the first order longitudinal mode, the resonance at ~96.1 x 10^3 rad./s corresponding to the second order flexural mode, and the resonance at ~42.1 x 10^3 rad./s corresponding to the first order flexural mode. With this model or the resonant modes, the speed of sound in the material was found to be (3291 ± 6) m/s. It's possible to make further predictions as to where resonant modes should fall, and further investigation into the resonance

of the piezoelectric sample would surely involve checking to see if predictions for higher order resonant modes hold.

In addition, two methods were used in modeling a particular resonance in greater detail. Analyzing the amplitude of oscillation yielded a resonance at $(131.5 \pm 0.1) \times 10^3$ rad./s with values for β, the damping coefficient, of $(2.60 \pm 0.10) \times 10^3$ rad./s and A, the force per mass coefficient, of $(839.0 \pm 21.6) \times 10^3$ m/s^2. Analyzing the shift in phase angle yields a resonance at $(130.44 \pm 0.01) \times 10^3$ rad./s with a damping coefficient of $(3.19 \pm 0.06) \times 10^3$ rad./s. Both methods used to determine these values produced similar results. However, they do not fall within each others' error values.

ACKNOWLEDGMENTS

I thank Judy Elwell and Ron Tebbe for their assistance.

[1] T. Ikeda, *Fundamentals of Piezoelectricity* (Oxford University Press, Oxford, 1990).

[2] S. T. Thornton and J. B. Marion, *Classical Dynamics of Particle and Systems* (Thomson, California, 2004) 5th ed.

[3] F. M. Mascarenhas, C. M. Spillman, J. F. Lindner, and D. T. Jacobs, Am. J. Phys. **66**, (1998), p. 692-697.